Construction of a Ground-Motion Logic Tree through Host-to-Target Region Adjustments Applied to an Adaptable Ground-Motion Prediction Model: An Addendum

David M. Boore[*1] (ID)

ABSTRACT

Boore et al. (2022; hereafter, Bea22) described adjustments to a host-region ground-motion prediction model (GMPM) for use in hazard calculations in a target region, using Chiou and Youngs (2014; hereafter, CY14) as the host-region model. This article contains two modifications to the Bea22 procedures for the host-to-target adjustments, one for the source and one for the anelastic attenuation function. The first modification is to compute logic-tree branches for the source adjustment variable Δc_M given in Bea22 assuming that the host- and target-region stress parameters are uncorrelated, instead of the implicit assumption in Bea22 that they are perfectly correlated. The assumption of uncorrelated stress parameters makes little difference for the example in Bea22 because the standard deviation of the host-region stress parameter is much less than that of the target-region stress parameter. However, this might not be the case in some future applications. The second modification is to the host-to-target anelastic attenuation path adjustment. The adjustment in Bea22 involves a distance-independent change in the γ variable that controls the rate of anelastic attenuation in the CY14 GMPM. This article proposes a method to account for a distance dependence in the adjustment. Such a dependence is needed for short-period ground-motion intensity measures (GMIMs) at distances greater than 100 km, with the importance increasing with distance. For the example in Bea22, the ratio of GMIMs computed with the revised and the previous adjustment to γ is less than about a factor of 1.05 at distances within about 100 km, but it can exceed a factor of 2 at 300 km for short-period GMIMs.

KEY POINTS

- Modifications are needed to the host-to-target adjustments suggested by Boore et al. (2022) (Bea22).
- Modifications to F_S assumes uncorrelated stress parameters and to F_A includes R dependence.
- Bea22 with modifications has been and is being used in high-level seismic hazard analyses globally.

INTRODUCTION

The ground motions needed for a probabilistic seismic hazard analysis (PSHA) are often based on adjusting a ground-motion prediction model (GMPM) developed for a host region to be applicable to a target region for which the PSHA will be calculated. As discussed in Bommer and Stafford (2020), this can be conveniently done by adjusting parameters on a backbone GMPM, particularly if that model uses functional forms that facilitate such adjustments. One such model is that of CY14, for which

$$\ln Y \sim F_S + F_A, \tag{1}$$

in which Y is a ground-motion intensity measure (GMIM; e.g., pseudo spectral acceleration [PSA] response spectra); F_S is an earthquake source function dependent on the moment magnitude **M**; and F_A is an anelastic attenuation function dependent on both source-to-site distance and earthquake magnitude. This process has inherent modeling, or epistemic, uncertainties

that must be accounted for in PSHA. Bea22 describes procedures for obtaining epistemic-uncertainty logic-tree branches for the host-to-target adjustments of F_S and F_A. The Bea22 procedures were used in a recently completed seismic hazard project at the Idaho National Laboratory (Idaho National Laboratory, 2022; hereafter, INL22).

This article discusses modifications to F_S and F_A that arose since the publication of Bea22. These modifications do not change the hazard calculated at the Idaho National Laboratory by the recent project, but they might be needed in future hazard calculations. The modification to F_S is an alternative method for using the uncertainty in the host-and-target $\Delta\sigma$ in computing the logic-tree branches of Δc_M, the parameter that controls the host-to-target adjustment of F_S. The modification to F_A allows the host-to-target adjustment parameter $\Delta\gamma$ to be a function of distance as well as magnitude.

MODIFICATION TO THE F_S HOST-TO-TARGET ADJUSTMENT

Bea22 shows how the source function in CY14 can be modified to account for host-to-target differences in the stress parameter. The modified source function is given by equation (2):

$$F_S = c_2(\mathbf{M} - 6) + \frac{c_2 - c_3}{c_n}\ln[1 + e^{c_n(c_M + \Delta c_M - \mathbf{M})}] - (c_2 - c_3)\Delta c_M,$$

(2)

in which

$$\Delta c_M = \chi_{FS2RS}\frac{2}{3}\log\frac{\Delta\sigma_T}{\Delta\sigma_H},$$

(3)

the logarithm is base 10; and χ_{FS2RS} is a period-dependent function (given in equations A17 and A18 in Bea22) that also depends on the sign of $\log\frac{\Delta\sigma_T}{\Delta\sigma_H}$. The coefficients c_2, c_3, c_n, and c_M in equation (2) are given in CY14.

If the cumulative distribution function (CDF) of Δc_M is known, then logic-tree branches for Δc_M can be determined using an approximation to the CDF. The one used in Bea22 was the Miller and Rice (1983) five-level approximation, for which the CDF levels are 0.034893, 0.211702, 0.500000, 0.788298, and 0.965107, with weights of 0.101080, 0.244290, 0.309260, 0.244290, and 0.101080 for branches 1–5, respectively.

A CDF for Δc_M was never determined explicitly in Bea22. Instead, the logic-tree branches for Δc_M were computed from the CDFs of $\Delta\sigma_H$ and $\Delta\sigma_T$. Because its uncertainty is so small, the CDF for $\Delta\sigma_H$ was a lognormal distribution given by the mean and standard deviation of $\ln\Delta\sigma_H$, using values in table 1 of Stafford et al. (2022; hereafter, Sea22). The CDF for $\Delta\sigma_T$ was obtained from a simulation procedure described in Bea22. This procedure involves fitting a bilinear stress parameter versus magnitude function to stress parameters in many simulated datasets (4000 in Bea22). The simulated datasets

were constructed by adding random noise to the dataset obtained from inversions of real data in the target region, using the uncertainty in the stress parameter for each event in the dataset. Following Sea22, the bilinear function for $\mathbf{M} \geq 5.0$ was flat, and the level of the stress parameter for this flat portion ($\Delta\sigma_{\mathbf{M}5}$) is the critical parameter in determining the host-to-target adjustment of the CY14 source function. For each simulated dataset, a CDF of $\Delta\sigma_T$ was constructed using the mean and standard error of $\Delta\sigma_{\mathbf{M}5}$ assuming a lognormal distribution, and the CDFs for all simulated datasets were then averaged to find the final CDF of $\Delta\sigma_T$. For the stress parameters used as an example in Bea22, Q–Q plots show the final CDF to be lognormally distributed for values of $\Delta\sigma_T$ within about 1.5 standard deviations of the median value. The CDFs for $\Delta\sigma_H$ and $\Delta\sigma_T$ were approximated by the five-point Miller and Rice representation. The logic-tree branches for Δc_M were then computed by substituting the $\Delta\sigma_H$ and $\Delta\sigma_T$ for the same Miller and Rice level into equation (3), one level at a time. This is equivalent to assuming perfect correlation of $\Delta\sigma_H$ and $\Delta\sigma_T$. If, on the other hand, $\Delta\sigma_H$ and $\Delta\sigma_T$ are uncorrelated, it is straightforward to construct a CDF for Δc_M using the known CDFs of $\Delta\sigma_H$ and $\Delta\sigma_T$, as obtained using the Bea22 procedures described in this paragraph. These CDFs can be sampled independently to obtain many pairs of uncorrelated host- and target-region stress parameters; substituting these pairs into equation (3) and ordering the results will yield a CDF of Δc_M. This does not assume that Δc_M has a normal distribution. This CDF can then be sampled using a finite-level approximation to obtain the values of Δc_M for the logic-tree branches. This is an addendum to the procedure described in Bea22.

Although the procedures just described can be used to construct logic-tree branches for Δc_M if $\Delta\sigma_H$ and $\Delta\sigma_T$ are uncorrelated or are perfectly correlated, it is instructive to consider a simplification if it is assumed that Δc_M has a normal distribution. To do this, it is convenient to write equation (3) in terms of the natural logarithm (because that is what is used in the CY14 GMPM) and expand the logarithm of the stress-parameter ratio into two terms, as follows:

$$\Delta c_M = \chi_{FS2RS}\frac{2}{3}(\log e)(\ln\Delta\sigma_T - \ln\Delta\sigma_H).$$

(4)

With the assumption that Δc_M has a normal distribution, the Δc_M for the logic-tree branches are the values corresponding to the desired levels of the CDF of Δc_M. These values can be obtained if the mean $\overline{\Delta c_M}$ and standard deviation σ of Δc_M are known. For example, the CDF levels for the five-level approximation of Miller and Rice (1983) are 0.034893, 0.211702, 0.500000, 0.788298, and 0.965107 (these were used in Bea22), and the Δc_M corresponding to these levels are given by adding -1.813σ, -0.801σ, -0.000σ, 0.801σ, and 1.813σ to $\overline{\Delta c_M}$.
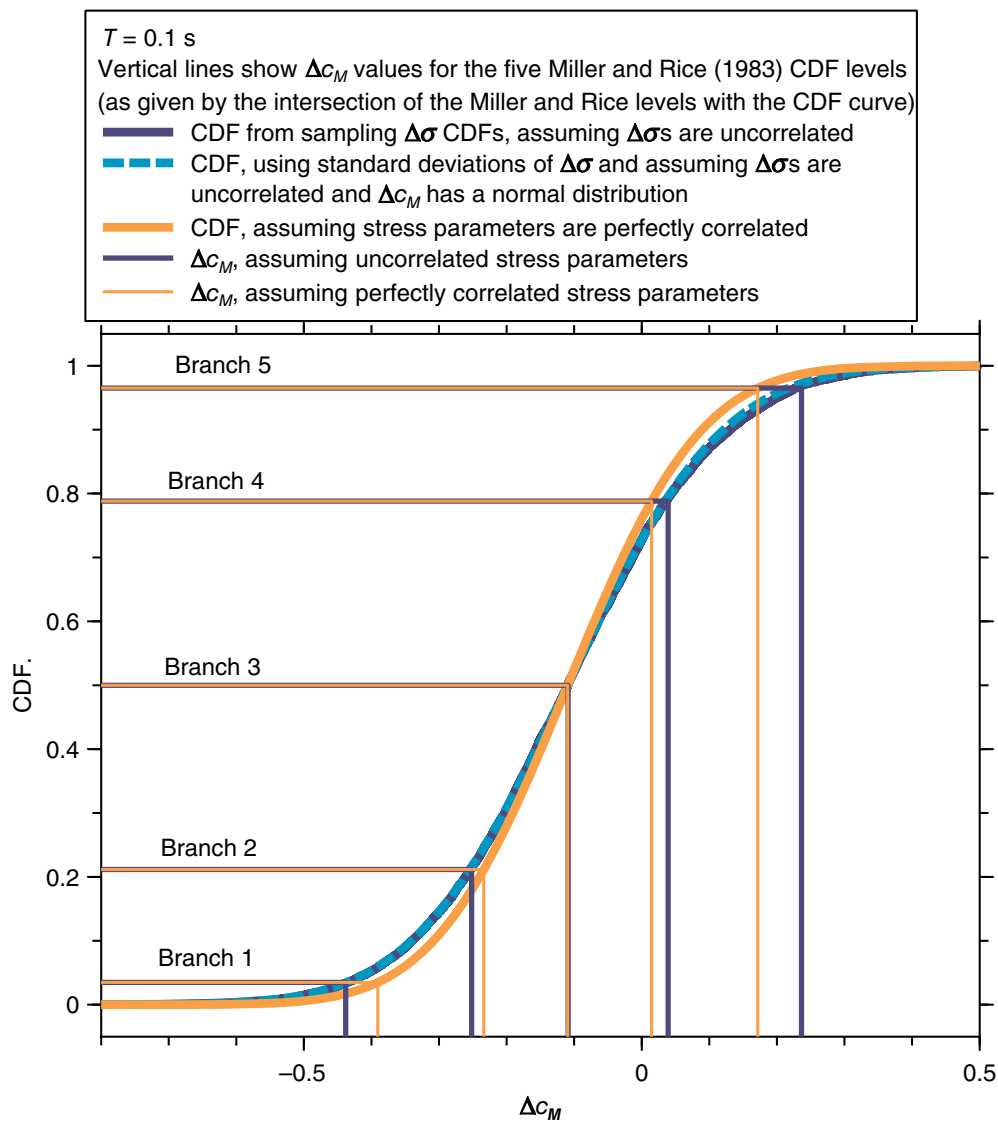
Figure 1. The cumulative distribution function (CDF) of Δc_M and the values for the logic-tree branches for 1 s pseudo spectral acceleration [PSA(0.1 s)] computed in various ways (see legend and Modification to the F_s Host-to-Target Adjustment section). The horizontal lines are the five-level Miller and Rice (1983) approximation to the CDF. The Sea22 value for the standard deviation of $\ln \Delta \sigma_H$ ($sd(\ln \Delta \sigma_H)$) for the host region (0.031) was used in the adjustment, and the value for $sd(\ln \Delta \sigma_T)$ used for the dashed line was that used in Bea22 (0.233). The color version of this figure is available only in the electronic edition.

in which $\xi_T = sd(\ln \Delta \sigma_T)$, $\xi_H = sd(ln\Delta \sigma_H)$, and ρ_{TH} is the correlation coefficient between $\ln \Delta \sigma_T$ and $\ln \Delta \sigma_H$. If the target- and host-region stress parameters are uncorrelated, $\rho_{TH} = 0$ and

$$sd(\ln \Delta \sigma_T - \ln \Delta \sigma_H)$$
$$= \sqrt{\xi_T^2 + \xi_H^2}. \qquad (7)$$

The other extreme is that the two stress parameters are perfectly correlated, in which case $\rho_{TH} = 1$, and

$$sd(\ln \Delta \sigma_T - \ln \Delta \sigma_H)$$
$$= \xi_T - \xi_H. \qquad (8)$$

If the host- and target-region stress parameters are determined independently, as is usually the case (e.g., in the INL Senior Seismic Hazard Analysis Committee level 3 study used in Bea22), equation (7) is the proper equation for determining the logic-tree branches of Δc_M using the simplified procedure if Δc_M is assumed to have a normal distribution.

To illustrate the various procedures for determining the logic-tree branches of Δc_M, Figure 1 shows the Δc_M CDFs and associated logic-tree values computed in several ways:

The mean of Δc_M is given using the means of $\ln \Delta \sigma_T$ and $\ln \Delta \sigma_H$ in equation (4). The standard deviation of Δc_M can be written as follows:

$$sd(\Delta c_M) = \chi_{FS2RS} \frac{2}{3} \log e \, sd(\ln \Delta \sigma_T - \ln \Delta \sigma_H), \qquad (5)$$

in which "$sd()$" stands for "standard deviation of the terms inside the parentheses". The standard deviation of the difference in $\ln \Delta \sigma$ depends on the correlation of $\Delta \sigma_T$ and $\Delta \sigma_H$, according to equation (6):

$$sd(\ln \Delta \sigma_T - \ln \Delta \sigma_H) = \sqrt{\xi_T^2 + \xi_H^2 - 2\rho_{TH}\xi_T\xi_H}, \qquad (6)$$

1. the addendum to Bea22 proposed in this article, in which independently sampled CDFs of $\Delta \sigma_T$ and $\Delta \sigma_H$ are used to construct the CDF of Δc_M; and

2. the simplified procedure that assumes a normal distribution for Δc_M and uncorrelated stress parameters (in this case, the standard deviation of $\Delta \sigma_T$ needed for this calculation is obtained by averaging the approximate σs obtained by dividing $\Delta \sigma_T$ for each Miller and Rice level by the equivalent number of standard deviations—1.813, 0.801, 0.801, and 1.813 for levels 1, 2, 4, and 5, respectively); and

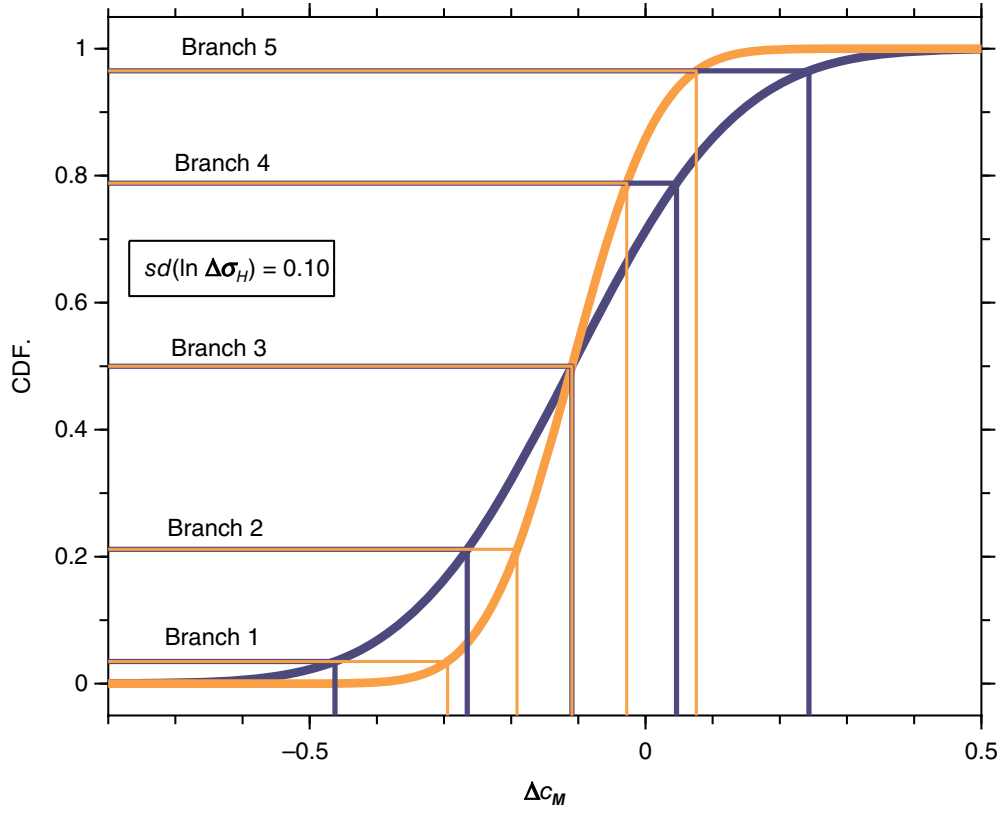3. the Bea22 procedure, assuming perfectly correlated stress parameters.

Figure 2. The CDF of Δc_M and the values for the logic-tree branches for PSA(0.1 s), assuming that the host- and target-region stress parameters are uncorrelated or are perfectly correlated. The horizontal lines are the five-level [Miller and Rice (1983)](#) approximation to the CDF. A value of 0.1 was used for the standard deviation of $ln\Delta\sigma_H$ for the host region ($sd(\ln\Delta\sigma_H)$) in the adjustment, whereas the value for $sd(\ln\Delta\sigma_T)$ was that used in Bea22 (0.233). The color version of this figure is available only in the electronic edition.

small differences in the logic-tree branches computed using either equation (7) or equation (8): $sd(\ln\Delta\sigma_T - \ln\Delta\sigma_H) = 0.235$ and 0.202 for equations (7) and (8), respectively. The standard deviation for the host-region stress parameter was small because it was from the inversion of the CY14 GMPM by Sea22; on the other hand, the target-region stress parameter came from the inversion of a sparse data set, resulting in a large standard deviation. To demonstrate the dependence of the results on the standard deviation of $\Delta\sigma_H$ when the stress parameters are assumed to be perfectly correlated, Figure 2 shows the results of procedures 2 and 3 when the value of $sd(\ln\Delta\sigma_H)$ was increased from 0.031 to 0.100. This was done to illustrate the sensitivity of the logic-tree branches to the relative sizes of the standard deviations of $\Delta\sigma_H$ and $\Delta\sigma_T$. The standard deviation of $sd(\ln\Delta\sigma_T - \ln\Delta\sigma_H)$ is now 0.254 and 0.133 for the uncorrelated and perfectly correlated cases, respectively, compared with 0.235 and 0.202 before. The consequence is that the spread of the Δc_M branches increases slightly for the uncorrelated case, and decreases significantly for the perfectly correlated case.

The results for the first two procedures—both of which assume uncorrelated host- and target-region stress parameters—are almost identical, probably because the distributions of the stress parameters are close to being normal. However, this may not always be the case and I recommend using procedure 1, which involves computing a CDF of Δc_M from the CDFs of $\Delta\sigma_T$ and $\Delta\sigma_H$.

The other interesting result in Figure 1 is that the logic-tree values of Δc_M are similar for both extreme assumptions of the stress parameters: perfectly correlated (as in Bea22) or uncorrelated. The reason for the similar results is that in the example used in Bea22, $sd(\ln\Delta\sigma_H)$ is much smaller than $sd(\ln\Delta\sigma_T)$ (0.031 and 0.233, respectively), so there are only

If the host- and target-region stress parameters were assumed to be perfectly correlated and both had the same standard deviation, the five values of Δc_M would coalesce into that for the middle branch; formally, there would be no epistemic uncertainty in Δc_M, an unrealistic result.

MODIFICATION TO THE F_A HOST-TO-TARGET ADJUSTMENT
Details of the modification
The modified CY14 backbone-model function for F_A is given by the following equation:

$$F_A = (\gamma + \Delta\gamma)R_{\mathrm{RUP}}, \qquad (9)$$

in which R_{RUP} is the closest distance from the rupture surface to the site, and

$$\gamma = c_{\gamma1} + \frac{c_{\gamma2}}{\cosh[\max(\mathbf{M} - c_{\gamma3}, 0)]}. \quad (10)$$

CY14 contains the values of the coefficients $c_{\gamma1}$, $c_{\gamma2}$, and $c_{\gamma3}$. The computation of $\Delta\gamma$ is discussed in this section.

In the procedure described in Bea22 for obtaining the logic-tree branches of $\Delta\gamma$, response spectra (PSA) are simulated for many magnitudes and distances, for each period of interest. The simulations are done for both the host and target regions, using the point-source stochastic model (Boore, 2003). This procedure requires the specification of the Fourier spectrum of the GMIM of interest (PSA, in this case). In Bea22, the Fourier acceleration spectrum (FAS) model developed by Sea22 was used for the simulations in both regions, the only difference being the Q parameters, which are region dependent. Following the procedure adopted in the Bea22 analysis, the uncertainties in the Q parameter are used to generate 1000 sets of those parameters, taking into account the correlation of the parameters. The PSA simulations are done for each set of Q parameters. The simulated PSAs for the two regions are converted to an adjustment to γ, using equation (11):

$$\Delta\gamma_{SIM} = \ln\left(\frac{PSA_T}{PSA_H}\right)/R_{RUP}. \quad (11)$$

Figure 3 is an illustration of the steps used in computing $\Delta\gamma_{SIM}$, for the host and region models used in Bea22. Figure 3a shows the Q values for the two regions, for two magnitudes (Q is a function of magnitude because the power of frequency in the computation of Q is a function of magnitude). Q for the target region is less than for the host region except for frequencies less than about 0.5 Hz, and therefore the simulated PSA for the target region will be less than for the host region except for oscillator periods (T) less than about 2 s. The simulated PSAs for both regions are shown in Figure 3b, for $T = 0.1$ s. The natural logarithm of the ratio of the target- and host-region PSAs are displayed in Figure 3c, and Figure 3d shows $\Delta\gamma_{SIM}$ computed from equation (11).

The simulations are done for a set of R_{JB} distances (the closest horizontal distance from the site to the surface projection of the fault-rupture plane), rather than R_{RUP} because it is convenient (but not essential) for $\Delta\gamma$ to be obtained at a magnitude-independent set of distances. The conversion from R_{JB} to R_{RUP} uses equation (12). This assumes a vertically dipping fault, which was the assumption used in the Sea22 development of the FAS model consistent with the CY14 GMPM.

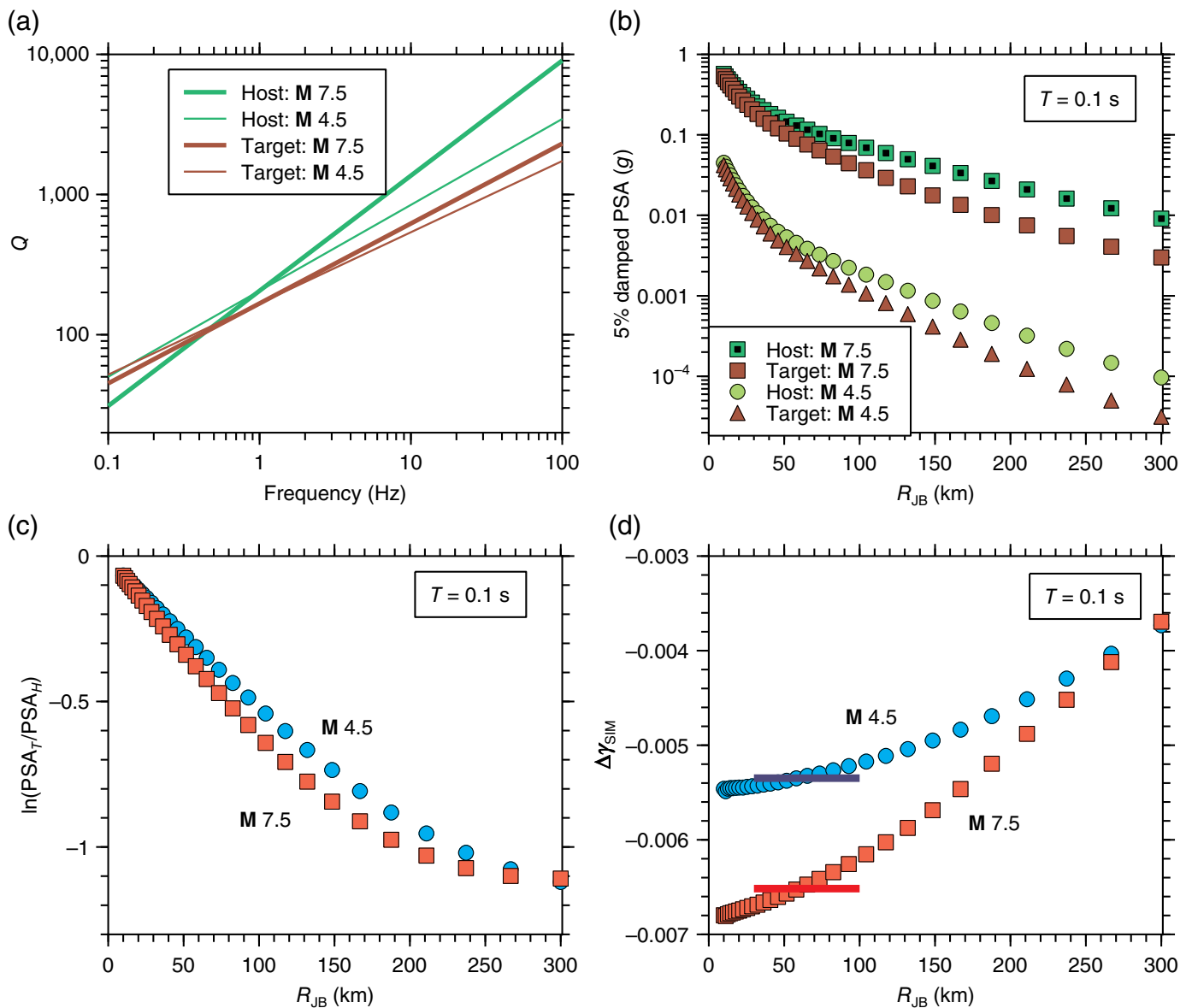$$R_{RUP} = \sqrt{R_{JB}^2 + Z_{TOR}^2}, \quad (12)$$

with Z_{TOR} (depth to top of rupture) being given by equation (5) in CY14; Z_{TOR} is a function of $\mathbf{M}$, thus making the set of R_{RUP}

determined from R_{JB} dependent on $\mathbf{M}$. For each period, there are $n_{SIM} \times n_M \times n_R$ values of $\Delta\gamma_{SIM}$, in which n_{SIM}, n_M, and n_R are the number of simulations, magnitudes, and distances, respectively. In the Bea22 procedure, $\Delta\gamma_{SIM}$ was averaged over distances from 30 to 100 km for each period, magnitude, and simulation, and the mean and standard deviations of these averages were computed over all the simulations. This distance range was used because most of the probabilistic seismic hazard for the target region used as an example in Bea22 came from source-to-site distances less than 100 km. Figure 3d shows the $\Delta\gamma_{SIM}$ and the average over distance used in Bea22, for a period of 0.1 s and two magnitudes. The mean and standard deviations of $\Delta\gamma$ were used to compute the logic-tree branches, assuming a normal distribution for $\Delta\gamma$ and using the Miller and Rice approximation to the implied CDF.

Although ignored in Bea22, Figure 3d shows that $\Delta\gamma$ is dependent on distance. To study this in more detail, the simulations were extended to greater distances and more periods than used in Bea22 (120 km and 0.1 s were used in Bea22). An example of the $\Delta\gamma$ adjustments from the new simulations are shown in Figure 4. Plotted are the means over the 1000 simulations ($\Delta\gamma_{SIM}$) for a set of distances, two magnitudes (4.5 and 7.5), and four oscillator periods (0.01, 0.1, 1.0, and 10.0 s). There is a clear dependence of $\Delta\gamma$ on distance for the shorter-period response spectra. The path adjustment for PSA is given by the exponentiation of $\Delta\gamma$ multiplied by R_{RUP} (equation 9), so using an average $\Delta\gamma$ of from 30 to 100 km instead of a distance-dependent value will lead to differences in PSA that increase with distance. This might not be a problem if the hazard is controlled by sources at short distances, but if more distant sources are important, then a distance dependence should be included in $\Delta\gamma$. This can be done using the procedure described in the next paragraphs.

Using the means and standard deviations over all simulations of $\Delta\gamma_{SIM}$ at each set of periods, magnitudes, and distances, the values corresponding to the logic-tree branches are computed using the procedure discussed earlier in this section. The adjustments to γ are then a function of $\mathbf{M}$, R_{RUP}, B (the logic-tree branch number), and T (the oscillator period) as indicated in this notation: $\Delta\gamma(\mathbf{M}, R_{RUP}|B, T)$, although the B and T dependence is assumed in the subsequent discussion and not shown explicitly, with a few exceptions. Furthermore, for simplicity the notation for $\Delta\gamma$ is sometimes used without arguments. In applications, these results could be expressed as a table lookup of $\Delta\gamma$ for a grid of $\mathbf{M}$ and R_{RUP}, for each branch and each period. However, this can be unwieldy, so a method was devised to approximate the results, using a polynomial fit of $\Delta\gamma$ versus distance for each $\mathbf{M}$, logic-tree branch, and period, followed by a polynomial fit of the distance-regression coefficients as a function of $\mathbf{M}$.

Based on plots such as shown in Figure 4, it was determined that a subset of five distances ($R_{JB} = 30$, 90, 150, 210, and 270 km for this example, shown by large symbols in Fig. 4)

(a)

(b)

(c)

(d)

Figure 3. Steps in deriving $\Delta\gamma$. (a) The Q functions for the host (CY14, from the Sea22 inversion) and target (INL) regions, shown for two magnitudes. (b) Simulated PSA as a function of distance for two magnitudes, using the host- and target-region Q models (the rest of the parameters used in the simulations were those for the host-region Fourier acceleration spectrum [FAS] model given by Sea22). (c) The natural logarithm of the ratio of PSA for the host (PSA_H) and target (PSA_T) regions. (d) The adjustment factor $\Delta\gamma_{SIM}$ for the path function F_A, as computed from equation (11). The short horizontal lines are the averages of $\Delta\gamma_{SIM}$ from 30 to 100 km, as used in Bea22. The color version of this figure is available only in the electronic edition.

and a second-order polynomial (quadratic) could be used for the fitting. A subset of distances is useful for computational efficiency because then the $\Delta\gamma$ for the logic-tree branches obtained from a large number of simulated motions at each distance needs to be computed for only a small fraction of the distances that otherwise might be considered. The second-order polynomial fit of $\Delta\gamma$ versus distance is given by equation (13):
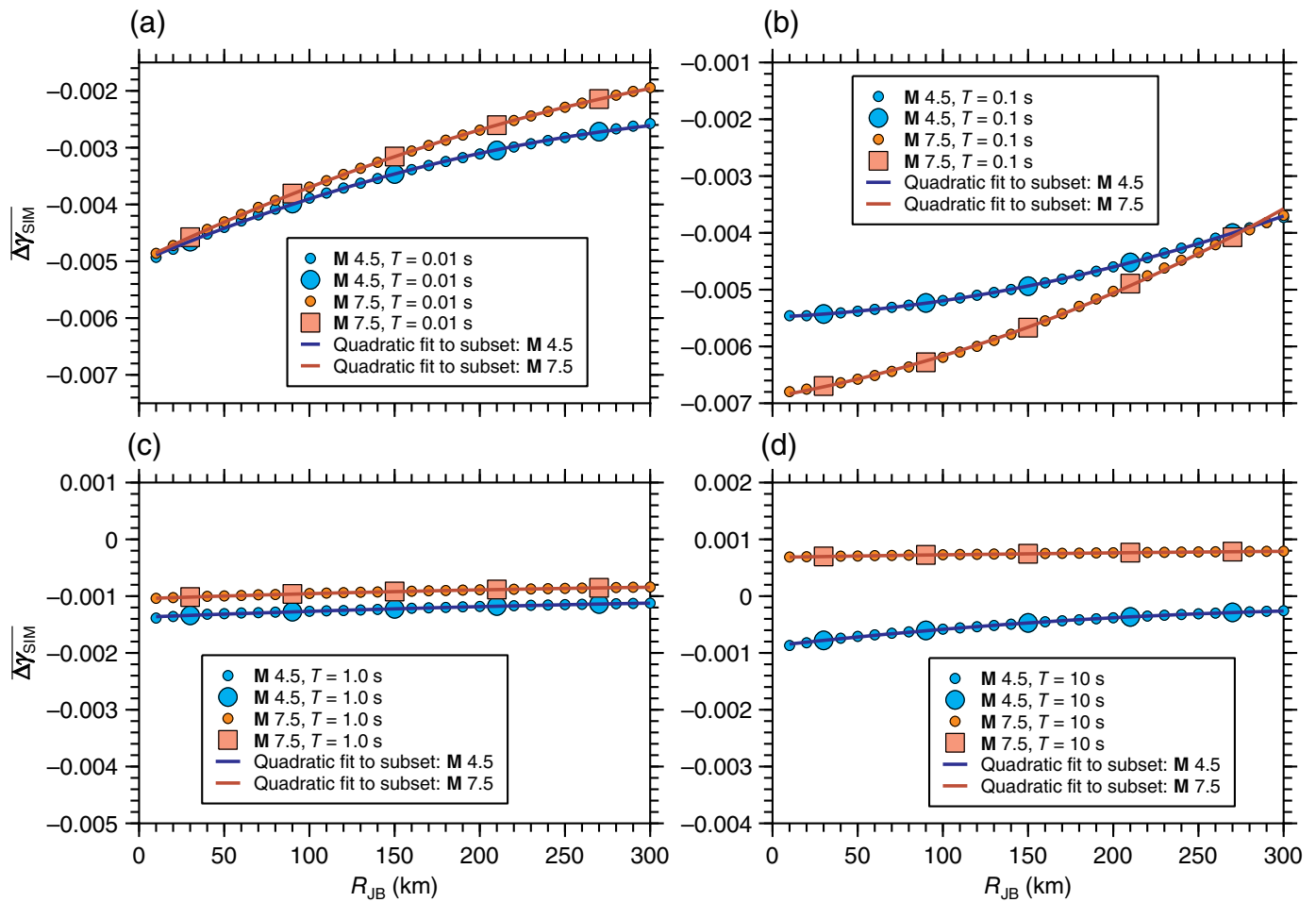
$$\widetilde{\Delta\gamma}(\mathbf{M},R_{\mathrm{RUP}}) = c_{0R}(\mathbf{M}) + c_{1R}(\mathbf{M})R_{\mathrm{JB}} + c_{2R}(\mathbf{M})R_{\mathrm{JB}}^2, \quad (13)$$

in which c_{0R}, c_{1R}, and c_{2R} are the regression coefficients for each magnitude $\mathbf{M}$. As it is clear from Figure 4, this polynomial provides a good fit to the distance dependence of $\Delta\gamma_{\mathrm{SIM}}$ using a small subset of the points.

The next step in the process is to fit each of the coefficients in equation (13) with a polynomial in $\mathbf{M}$. Various functions were tried; reasonable fits for a wide range of periods were obtained using a third-order (cubic) polynomial. The results

are shown in Figure 5. There is more variation in the trends of the distance-regression coefficients with magnitude than there was for $\Delta\gamma(\mathbf{M},R_{\mathrm{RUP}})$ as a function of distance for a fixed $\mathbf{M}$ (compare Figs. 4 and 5). The equations for the magnitude dependence of the distance-regression coefficients are:

Panel labels: (a), (b), (c), (d)

Panel (a) legend:
- M 4.5, $T = 0.01$ s
- M 4.5, $T = 0.01$ s
- M 7.5, $T = 0.01$ s
- M 7.5, $T = 0.01$ s
- Quadratic fit to subset: M 4.5
- Quadratic fit to subset: M 7.5

Panel (b) legend:
- M 4.5, $T = 0.1$ s
- M 4.5, $T = 0.1$ s
- M 7.5, $T = 0.1$ s
- M 7.5, $T = 0.1$ s
- Quadratic fit to subset: M 4.5
- Quadratic fit to subset: M 7.5

Panel (c) legend:
- M 4.5, $T = 1.0$ s
- M 4.5, $T = 1.0$ s
- M 7.5, $T = 1.0$ s
- M 7.5, $T = 1.0$ s
- Quadratic fit to subset: M 4.5
- Quadratic fit to subset: M 7.5

Panel (d) legend:
- M 4.5, $T = 10$ s
- M 4.5, $T = 10$ s
- M 7.5, $T = 10$ s
- M 7.5, $T = 10$ s
- Quadratic fit to subset: M 4.5
- Quadratic fit to subset: M 7.5

Axis labels: $\overline{\Delta\gamma_{SIM}}$ (ordinate), R_{JB} (km) (abscissa)

Figure 4. $\overline{\Delta\gamma_{SIM}}$, the adjustment to the CY14 anelastic attenuation parameter γ, as a function of R_{JB} for four periods (panels a–d), and two magnitudes. For ease in comparing the magnitude and distance dependence for the different periods, the ordinate-axes scales are the same for the four graphs. $\overline{\Delta\gamma_{SIM}}$ is the mean over all simulations of $\Delta\gamma_{SIM}$ for each magnitude and distance. The large symbols show the subset of $\overline{\Delta\gamma_{SIM}}$ used to derive the regression coefficients for the revised γ adjustments discussed in this article, with the quadratic fit to this subset shown by the lines. If missing, axis titles or labels are those shown for labeled panels in the corresponding rows or columns. The color version of this figure is available only in the electronic edition.

$$\widetilde{c_{0R}}(\mathbf{M}) = c_{0M0R} + c_{1M0R}\mathbf{M} + c_{2M0R}\mathbf{M}^2 + c_{3M0R}\mathbf{M}^3, \quad (14a)$$

$$\widetilde{c_{1R}}(\mathbf{M}) = c_{0M1R} + c_{1M1R}\mathbf{M} + c_{2M1R}\mathbf{M}^2 + c_{3M1R}\mathbf{M}^3, \quad (14b)$$

$$\widetilde{c_{2R}}(\mathbf{M}) = c_{0M2R} + c_{1M2R}\mathbf{M} + c_{2M2R}\mathbf{M}^2 + c_{3M2R}\mathbf{M}^3. \quad (14c)$$

Once the coefficients in equations (14a), (14b), and (14c) have been determined (in the example in this article, 12 coefficients for each logic-tree branch and period), the CY14 anelastic attenuation path function for the target region is given by the following equation:

$$F_A = (\gamma + \widetilde{\Delta\gamma}(\mathbf{M}, R_{RUP}|B, T))R_{RUP}, \quad (15)$$

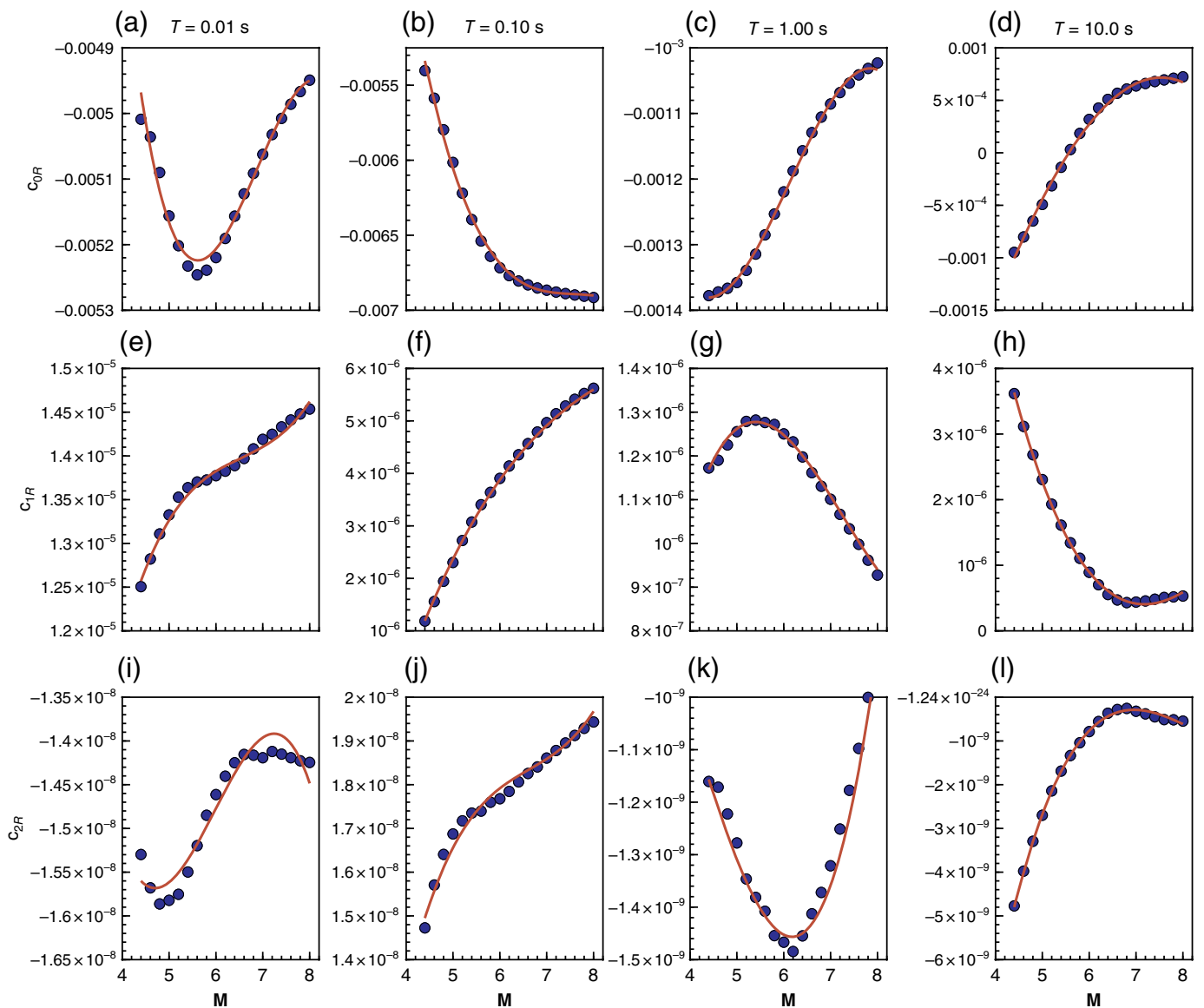in which $\widetilde{\Delta\gamma}(\mathbf{M}, R_{RUP}|B, T)$ is determined by first evaluating equations (14a), (14b), and (14c) to obtain approximations of the distance-regression coefficients ($\widetilde{c_{iR}}$, with $i = 0$, 1, and 2 for the example in this article) for a given $\mathbf{M}$, and these approximations for the distance coefficients are then used in equation (13).

To check the procedure, Figure 6 compares $\widetilde{\Delta\gamma}$ from the approximate procedure (equations 13 and 14) with $\Delta\gamma$. It is clear that $\widetilde{\Delta\gamma}$ from the approximate procedure, based on distance- and magnitude regressions, is in excellent agreement with $\Delta\gamma$.

Consequences of the modification

Although the distance dependence in the revised procedure to determine $\Delta\gamma$ can be inferred from Figure 6, the independent ordinate-axis scaling for the graphs in the figure can distort the importance of the dependence. For example, for a period of 1.0 s there appears to be a significant distance dependence, but the absolute difference in $\Delta\gamma$ from 30 to 270 km is close to 0.0002 natural log units, which is a factor of 10 smaller than

Figure 5. (a–l) The symbols are the distance-regression coefficients computed from equation (13), and the curves show the cubic polynomial fit to the distance coefficients as a function of magnitude from equations (14a), (14b), and (14c), for the middle logic-tree branch. The graphs in each row correspond to the coefficient identified in the ordinate-axis title at the left of each row, and the graphs in each column correspond to the oscillator period identified at the top of each column. The ordinate-axis scales are chosen separately for each graph, to facilitate the visual inspection of the cubic polynomial fits to the distance-regression coefficients. If missing, axis titles or labels are those shown for labeled panels in the corresponding rows or columns. The color version of this figure is available only in the electronic edition.

the maximum difference for a period of 0.1 s. An easier way of assessing the importance of the distance dependence in $\Delta\gamma$ is given in Figure 7, which shows $\Delta\gamma$ as a function of magnitude for one period (0.1 s) and three distances: 30, 58, and 100 km. $\Delta\gamma$ in the figure is for the middle branch of the logic tree, as computed using the method described in the section immediately preceding this section. The distance-independent $\Delta\gamma$ of Bea22 (shown in Fig. 3d) is the same as for the $R_{JB} = 58$ km curve. If that curve had been used to compute the host-to-target adjustment to the anelastic path function for **M** 7.5 and for a site at 100 km, Figure 7 shows that the host-to-target adjustment to γ would have been too low by 0.00035 natural log units. This is equivalent to a factor of $\exp(0.00035 \times 100) = 1.036$ in the ratio of the GMIM at 100 km computed using the previous and revised host-to-target adjustment to the anelastic attenuation path function.

Although Figure 7 is informative, a more direct view of the consequences of the revised host-to-target adjustment to the

anelastic attenuation path function is to show the ratio of the GMIM Y for the previous and revised procedures for obtaining the adjustment. Let Y_H and Y_T be the portions of the GMIMs for the host and the target regions that are attributable to the anelastic attenuation path function. Then from equations (1) and (15), the multiplicative factor χ_{F_A} that converts Y_H to Y_T is given by the following equation:
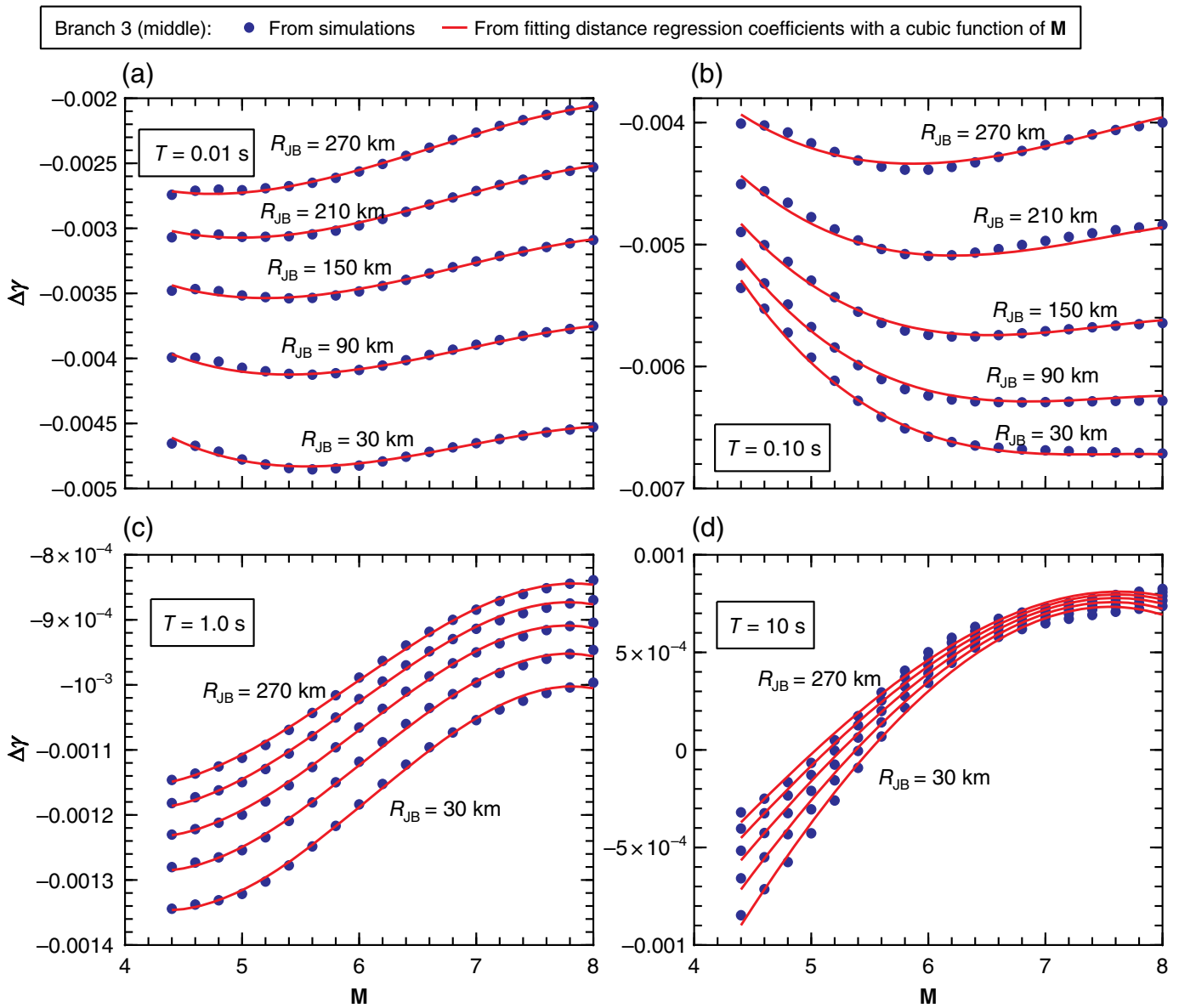
Figure 6. The anelastic attenuation adjustment parameter $\Delta\gamma$ for the middle branch of the logic tree, from the simulations ($\Delta\gamma$, given by the symbols) and from the combination of fitting the simulations with a regression over distance, followed by a regression of the distance-regression coefficients over magnitude ($\widetilde{\Delta\gamma}$, given by the lines). The comparison is shown as a function of magnitude for four oscillator periods and five distances. The ordinate-axis scales are chosen separately for each plot; the range of $\Delta\gamma$ is wider for the short periods ((a) 0.01 and (b) 0.1 s) than it is for the longer periods ((c) 1.0 and (d) 10 s). If missing, axis titles or labels are those shown for labeled panels in the corresponding rows or columns. The color version of this figure is available only in the electronic edition.

$$\chi_{F_A} = \frac{Y_T}{Y_H} = \exp(\widetilde{\Delta\gamma}R_{\text{RUP}}). \tag{16}$$

Figure 8 shows χ_{F_A} plotted against R_{RUP} for four periods, including the extreme periods used in CY14 (0.01 and 10.0 s). The results are shown for one magnitude (7.0) and the lowest, middle, and highest logic-tree branches ($B = 1$, 3, and 5). The results for other magnitudes, ranging from 4.5 to 8.0, are similar in appearance. The results are shown both for the Bea22 (distance-independent, as given using $\Delta\gamma$ at 58 km) and the revised (distance-dependent) adjustments to γ. Consistent with the example discussed in the previous paragraph, the differences using the two ways of computing the adjustment are relatively minor for distances within about 100 km. The differences are also minor for longer periods at all distances, but they can be substantial for short periods, with the importance growing with distance. For example, for a period of 0.1 s at 300 km, Y_T from the revised $\Delta\gamma$

would be a factor of 2.0 times larger than if it had been computed using the Bea22 procedure to determine $\Delta\gamma$. The adjustments are negative for all periods but 10 s. This is consistent with the Q values shown in Figure 3a, which result in the target-region attenuation being greater than the host-region
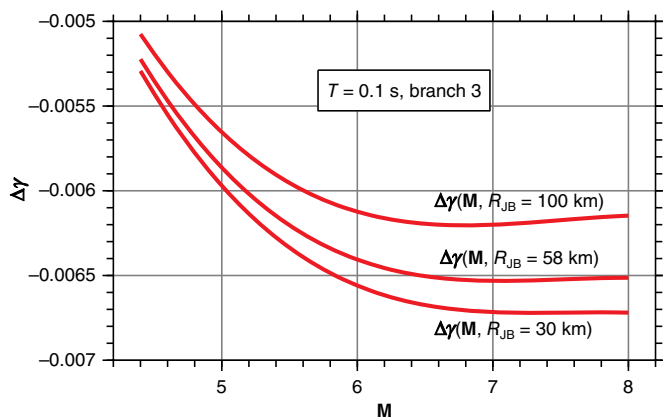
Figure 7. $\Delta\gamma$ versus **M** for $T = 0.1$ s for the middle logic-tree branch (branch 3) for three values of R_{JB}. Although not shown to avoid clutter in the figure, the relative differences in $\Delta\gamma$ for the three distances is similar for the other logic-tree branches. The color version of this figure is available only in the electronic edition.

attenuation except for frequencies less than about 0.5 Hz and **M** 7.5 (although not shown in Figure 3a, the Q values for **M** greater than about 6.5 are almost identical to those for **M** 7.5). The negative $\Delta\gamma$ adjustments lead to the target-region PSA being less than the host-region PSA, except for the oscillator responses at long periods.

DISCUSSION AND CONCLUSIONS

Bea22 discusses a number of host-to-target adjustments to a backbone GMPM used to compute seismic hazard in regions other than those from which the backbone model was derived. This article discusses modifications to two of those adjustments—for the earthquake source function and for the anelastic path function. For the source adjustment, a procedure to produce the CDF of the adjustment parameter Δc_M is given that assumes uncorrelated host- and target-region stress parameters (implicit in the Bea22 procedure is that the stress parameters are perfectly correlated); the logic-tree branches for Δc_M can be computed from the CDF. In the example used in Bea22, the uncertainty in the logarithm of the host-region stress parameter is so small (0.031) compared with that for the target region (0.233), that there is little change in the Δc_M logic-tree branches when the modification in this article is used. But for situations in which the host-region stress parameter has a larger uncertainty, there can be a significant difference in the Δc_M adjustment for all but the middle branch of the logic tree. It is my opinion that in most, if not all, applications, $\Delta\sigma$ for the host and target regions will be uncorrelated.

The other modification is to the Bea22 host-to-target adjustment $\Delta\gamma$ used in the CY14 anelastic attenuation path function. In Bea22, the adjustment used an average of simulations of the $\Delta\gamma$ adjustments over a range of distances from 30 to 100 km. Even though some variation with distance was
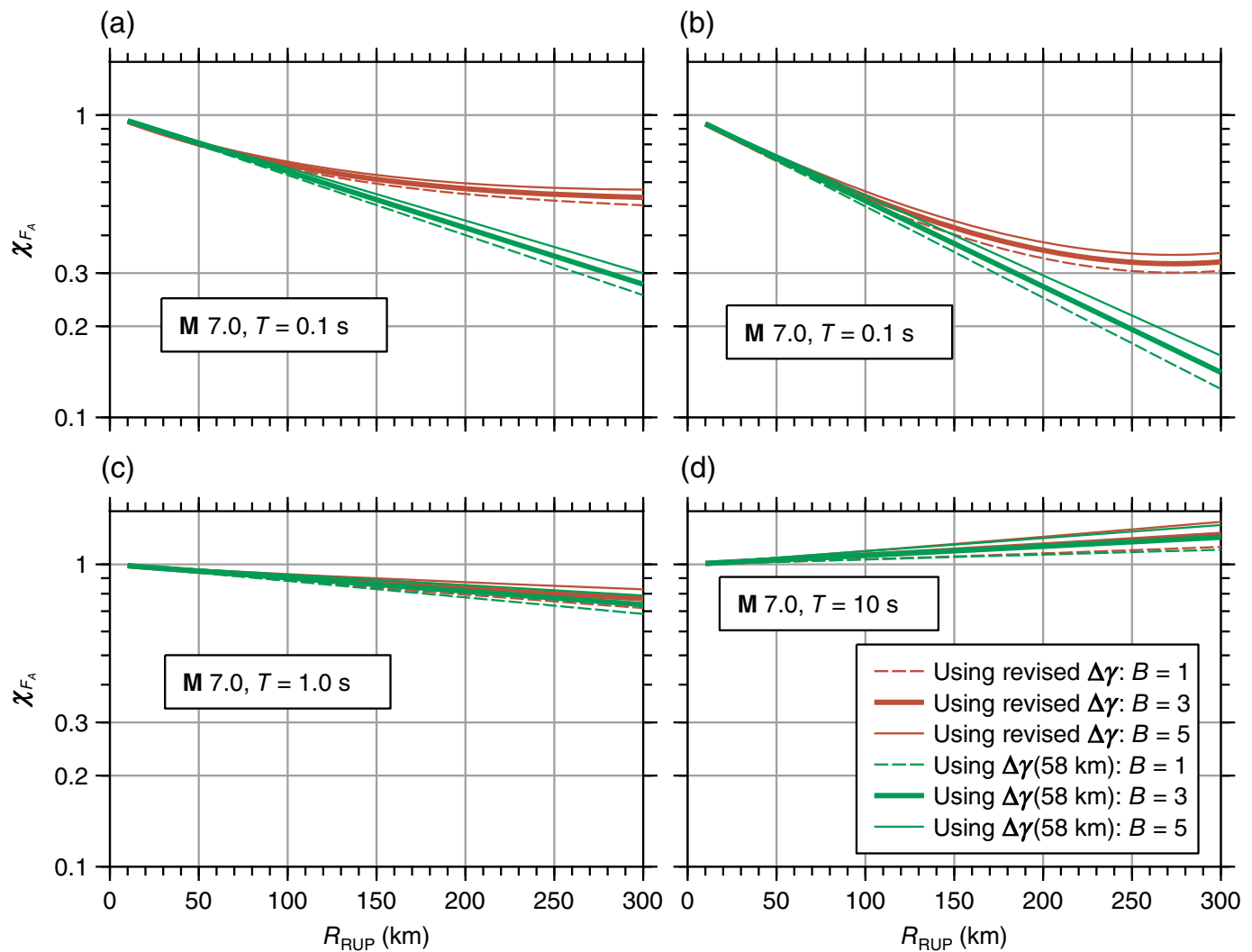
observed in the simulations of $\Delta\gamma$, this variation was ignored in the Bea22 procedure for computing the adjustment. Inspection of the simulations for short-period motions, however, finds a clear dependence of $\Delta\gamma$ with distance. This article proposes a procedure to include the distance dependence of $\Delta\gamma$. For a given period and logic-tree branch, the procedure uses regression fits to the distance dependence and the magnitude dependence of the simulated $\Delta\gamma$ over a grid of distance and magnitude values. This results in a convenient approximation of the distance and magnitude dependence of $\Delta\gamma$ given by 12 regression coefficients for a given logic-tree branch and period. The result is denoted $\widetilde{\Delta\gamma}(\mathbf{M}, R_{\mathrm{RUP}}|B, T)$, with the tilde used to indicate that the computed values are an approximation to the simulated values of $\Delta\gamma$. The approximated values are very close to the simulated values when compared over a wide range of magnitudes and distances. Comparisons of the host-to-target adjustments from the distance-independent and the distance-dependent $\Delta\gamma$ finds minor differences for longer periods (1.0 and 10 s in this article) at all distances and for shorter periods (0.01 and 0.1 s in this article) for distances less than about 100 km. This distance is only an approximation because the difference gradually increases with distance, becoming quite important for shorter periods at distances of hundreds of kilometers, where the ratio of GMIM computed using the revised and previous γ adjustments can exceed a factor of 2.

Both of the modifications to Bea22 discussed in this article used the FAS model for the CY14 host-region GMPM developed by Sea22, but the procedure can be adapted for use with other FAS models.

To close, I include here a few comments on the distance dependence of $\Delta\gamma$. That there is a dependence might come as a surprise at first glance. The only differences in the FAS models for the host and target regions are the Q values. Because Q enters the FAS model as

$$\mathrm{FAS} \propto \exp\left(-\frac{\pi f R_{\mathrm{RUP}}}{Q c_Q}\right), \qquad (17)$$

in which c_Q is an average shear-wave velocity used in the derivation of Q from observations, R_{RUP} cancels out of the equation for $\Delta\gamma$ if the FAS model is used in equation (11) instead of the PSA values. That there is an R_{RUP} dependence to $\Delta\gamma$ is related to response spectral values for a given oscillator period generally being determined by a range of frequencies in the Fourier spectra, as discussed, for example, by Bora *et al.* (2016) and Dujardin *et al.* (2016). This dependence can be difficult to predict simply by looking at plots of FAS, but some appreciation of the issue can be obtained from Figure 9, which shows a FAS model made up of the following contributions: a single-corner frequency ω^2 source model (S), a Q function (D, given by equation 17), a diminution function ($D = \exp[-\pi\kappa_0 f]$, in which $k_0 = 0.039$ s), and a 5% damped oscillator response

Figure 8. The multiplicative factor $\chi_{F_A} = \exp \Delta F_A$, in which $\Delta F_A = \widetilde{\Delta\gamma} R_{RUP}$ (see equations 15 and 16) for four periods (panels a–d), including the shortest (0.01 s) and longest (10.0 s) response spectral periods used in CY14. This factor converts the part of the host-region ground-motion intensity measure (GMIM) due to F_A (as given by $\exp \gamma R_{RUP}$) to the target region. χ_{F_A} is plotted versus R_{RUP} for two periods, one magnitude, and the lowest, middle, and highest logic-tree branches ($B = 1$, 3, and 5). χ_{F_A} was computed using both the revised, distance-dependent $\Delta\gamma$ and a distance-independent $\Delta\gamma$ given by evaluating the revised $\Delta\gamma$ at $R_{JB} = 58$ km. The ordinate-axis scales are the same for all graphs, to allow a better comparison of the adjustments for different periods. Note that the total path function in the CY14 ground-motion prediction model (GMPM) includes geometrical spreading and γR_{RUP} (equation 9); the contributions to the GMIM due to these functions are not shown in this figure, which is only concerned with the consequences of different ways of computing the host-to-target adjustments in the anelastic attenuation path function. If missing, axis titles or labels are those shown for labeled panels in the corresponding rows or columns. The color version of this figure is available only in the electronic edition.

with natural frequency given in the abscissa (O). Plotted is the square of the FAS as a function of linear frequency because it is this that is used in computing the spectral moments used in the random vibration theory for determining the value of the response spectral amplitudes (e.g., Boore, 2003). Figure 9 shows the combined FAS for two periods, 0.1 and 10.0 s, for two distances (20 and 100 km), and two regions (host and target). Recall that the only difference in the FAS models for the two regions in the derivation of $\Delta\gamma$ is in the Q values. The FAS for the short-period oscillator clearly has different shapes for the four curves, and because the PSA values come from integrals of the curves over frequency, it is not surprising that the ratios of host-to-target response spectra will be different for the two distances. This results in a distance dependence for $\Delta\gamma$. Here, the Q differences between the host- and target regions have a major influence on what is expected from Fourier versus response spectra, a point made by Dujardin *et al.* (2016). On the other hand, the FAS models for the long-period oscillator responses are much more similar in shape than for the short-period oscillator responses (as pointed out by Bora *et al.*, 2016), and therefore the results of using either FAS or the PSA values

in equation (11) should be similar, with much less distance dependence for $\Delta\gamma$ than for shorter periods, consistent with what is shown in Figure 8.
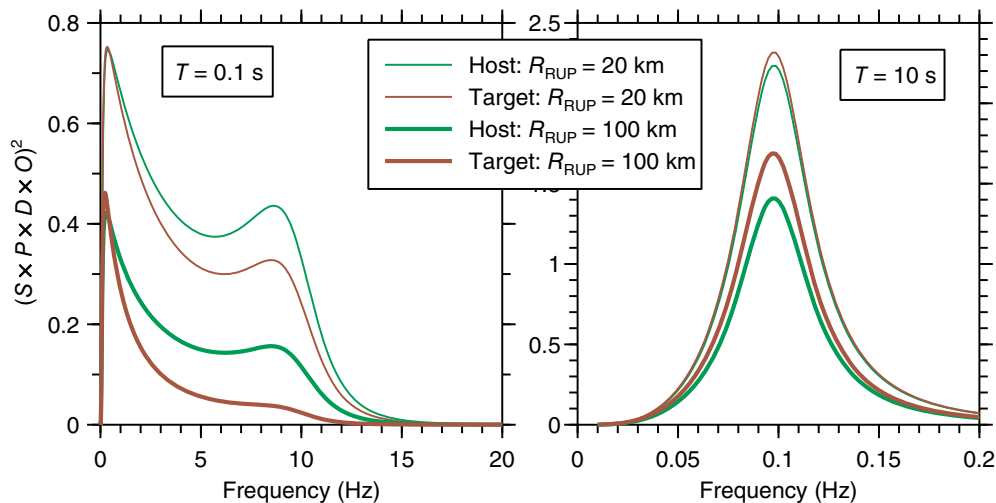
Figure 9. The combination of the source function for acceleration (S), Q function (P), κ_0 diminution function (D), and oscillator response (O) for **M** 7.5, $\Delta\sigma = 100$ bars, and $\kappa_0 = 0.039$ s. Shown is the square of the combination of factors (see Discussion and Conclusions section). Curves are shown for host- and target-region Q parameters, two distances (R_{RUP}), and two oscillator periods (T). The color version of this figure is available only in the electronic edition.

DATA AND RESOURCES

The figures were prepared using CoPlot available at www .cohortsoftware.com. Most of the analysis used scripts written in the statistical language and environment R (R Core Team, 2022) available at https://www.r-project.org/. All websites were last accessed in September 2023.

DECLARATION OF COMPETING INTERESTS

The author acknowledges that there are no conflicts of interest recorded.

ACKNOWLEDGMENTS

REFERENCES

Bommer, J. J., and P. J. Stafford (2020). Selecting ground-motion models for site-specific PSHA: Adaptability versus applicability, *Bull. Seismol. Soc. Am.* **110,** 2801–2815, doi: 10.1785/0120200171.

Boore, D. M. (2003). Prediction of ground motion using the stochastic method, *Pure Appl. Geophys.* **160,** 635–676.

Boore, D. M., R. R. Youngs, A. R. Kottke, J. J. Bommer, R. Darragh, W. J. Silva, P. J. Stafford, L. Al Atik, A. Rodriguez-Marek, and J. Kaklamanos (2022). Construction of a ground-motion logic tree through host-to-target region adjustments applied to an adaptable ground-motion prediction model, *Bull. Seismol. Soc. Am.* **112,** 3063–3080, doi: 10.1785/0120220056.

Bora, S. S., F. Scherbaum, N. Kuehn, and P. Stafford (2016). On the relationship between Fourier and response spectra: Implications for the adjustment of empirical ground-motion prediction equations (GMPEs), *Bull. Seismol. Soc. Am.* **106,** 1235–1253.

Chiou, B. S. J., and R. R. Youngs (2014). Update of the Chiou and Youngs NGA Model for the average horizontal component of peak ground motion and response spectra, *Earthq. Spectra* **30,** 1117–1153.

Dujardin, A., F. Courboulex, M. Causse, and P. Traversa (2016). Influence of source, path, and site effects on the magnitude dependence of ground-motion decay with distance, *Seismol. Res. Lett.* **87,** 138–148.

Idaho National Laboratory (2022). *Idaho National Laboratory Sitewide SSHAC Level 3 Probabilistic Seismic Hazard Analysis, INL/RPT-22-70233*, Idaho National Laboratory, Idaho Falls, Idaho.

Miller, A. C., and T. R. Rice (1983). Discrete approximations of probability distributions, *Manage. Sci.* **29,** 352–362.

R Core Team (2022). R: A language and environment for statistical computing, R Foundation for Statistical Computing, Vienna, Austria.

Stafford, P. J., D. M. Boore, R. R. Youngs, and J. J. Bommer (2022). Host-region parameters for an adjustable model for crustal earthquakes to facilitate the implementation of the backbone approach to building ground-motion logic trees in probabilistic seismic hazard analysis, *Earthq. Spectra* **38,** 917–949.